A Compact Model for Predicting the Isolation of Ports in a Closed Rectangular Microchip Package

Hilding M. Olson, *Life Member, IEEE*

Abstract— **This paper presents the derivation of a compact model for predicting the isolation between ports on opposite sides of a microchip package such as would be used for MMIC chips. The model consists of four current sources, two electric, and two magnetic, representing the port currents and voltages which excite the modes of a cavity formed by the interior of the package. The contribution of each mode to the total electric field is summed, and the average of the total tangential field along the two probes that project into the cavity at the ports is set equal to zero. The model, which runs on a PC, is used to compute data for an actual package, and the data is compared with that produced by a commercial electromagnetic analysis package running on a work station.**

I. Introduction

In designing microwave packages for MMIC chips it is very important to avoid signal contamination or signal feedback at the RF ports. Hence, the signal isolation between these ports must be kept high. Since it is advantageous to be able to predict the degree of isolation for a given design, a method of analyzing the coupling between ports of the package is needed. This paper describes an analytic method that satisfies this need and can be implemented on a PC.

These packages with their RF ports often closely resemble rectangular cavities with probe excitations. Several authors have analyzed such structures [1]–[3]. The model presented here serves for the class of package that approximates a rectangular cavity with shielded microstrip ports in opposite sides. The microstrip conductor extends into the cavity as a probe. Although the actual package configuration under consideration may differ appreciably from a purely rectangular cavity, this is a geometry that is reasonably simple to analyze and therefore useful for estimating the package isolation. And although the ports of the actual package may be different from shielded microstrip, this geometry also lends itself to simplicity of analysis. The geometry assumed for the analysis is shown in Fig. 1.

The approach to the computation of isolation is to take advantage of the equivalence principle [4] to replace the electromagnetic fields in the apertures of the ports by fictitious magnetic currents. These together with the electric currents flowing on the probes are the sources for the EM field in the cavity. With assumptions made for the spatial distribution of these currents, the amplitudes of the currents are found from the constraint that the average value of the tangential electric field along the probes must vanish.

Manuscript received January 30, 1995; revised October 2, 1995. This work was supported in part by a Grant from the Jet Propulsion Laboratory, California Institute of Technology, Pasadena, CA.
The author is with the Electrical Engineering and Computer Science Department, Lehigh University, Bethlehem, PA 18015 USA.
Publisher Item Identifier S 0018-9480(96)00476-0.

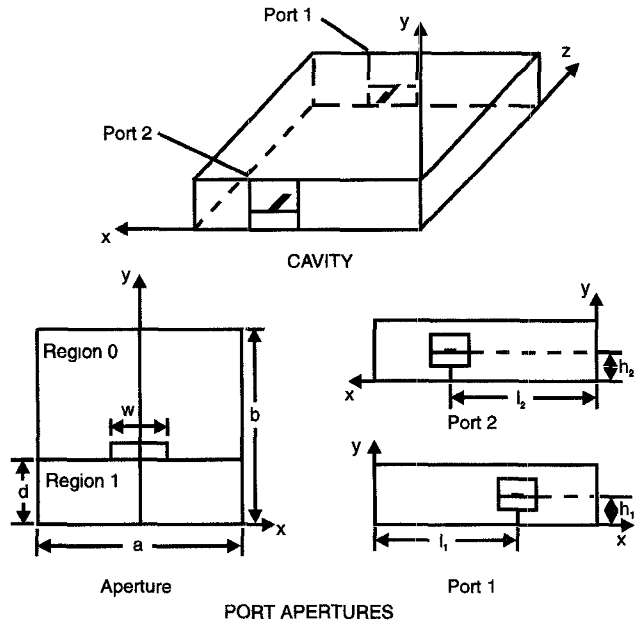

Fig. 1. Geometry of model.

An equation has been derived by Kisliuk [5] for the electric field inside a rectangular cavity in terms of sources within the cavity. The actual distribution of electric field in the aperture at the intersection of the shielded microstrip ports and the cavity is unknown. However, a reasonable approximation is to assume that the distribution does not differ much from the distribution of field over the cross section of a uniform infinitely long shielded microstrip line. Similarly, the distribution of current on the microstrip conductor projecting into the cavity is unknown. However, it is known to be higher at the edges of the strip than in the center. A reasonable assumption for the current distribution is a cosine-squared distribution across the width of the conductor and sinusoidal along its length. The latter assumption is widely used in cavity excitation problems [6], [7].

The unknown quantities to be solved for are the voltage on the port #2 microstrip and the currents on the two microstrip probes for an applied voltage of one volt on the port #1 microstrip. From these quantities one can then determine the S-parameters and the two-port insertion and return losses.

II. Derivation of Analytic Model

The E-field within a rectangular cavity can be expressed in terms of the cavity modes or eigenvectors and source currents within the cavity as [5]

$$\vec{E}(\vec{r}) = \sum_{\nu} \left\{ \kappa_\nu \begin{bmatrix} \left(\frac{k_\nu}{j\omega\varepsilon} J_{eM_\nu} - J_{mK_\nu}\right) W_{M_\nu} \vec{M}_\nu(\vec{r}) \\ + \left(\frac{k_\nu}{j\omega\varepsilon} J_{eN_\nu} - J_{mF_\nu}\right) W_{N_\nu} \vec{N}_\nu(\vec{r}) \end{bmatrix} \right\} - \frac{1}{j\omega\varepsilon} \vec{J}_e(\vec{r}) \tag{1}$$

where k_ν, the eigenvalue of mode ν, is given by $k_\nu^2 = k_x^2 + k_y^2 + k_z^2 = \omega_\nu^2 \varepsilon\mu$ and $k_0^2 = \omega^2\varepsilon\mu$ with

$$k_x = \frac{m\pi}{a}; \quad k_y = \frac{n\pi}{b}$$

and

$$k_z = \frac{p\pi}{c}.$$

The resonant frequency of mode ν is symbolized by ω_ν and the applied frequency by ω.

$$\kappa_\nu = \frac{k_\nu}{k_\nu^2 - k_0^2}$$

and

$$J_{eM_\nu} = \int_V \vec{M}_\nu(\vec{r}) \cdot \vec{J}_e(\vec{r})\, dV, \text{ etc.} \tag{2}$$

The final term in (1) arises when there are volume current densities in the cavity. For this model, in the absence of volume currents, this term is neglected. The TE^z and TM^z "electric" eigenvectors, $M_\nu(r)$ and $N_\nu(r)$, respectively, are given by

$$\vec{M}_\nu = \frac{1}{k_\nu} \vec{\nabla} \times (\vec{a}_z f_{M_\nu})$$

and

$$\vec{N}_\nu = \frac{1}{k_\nu^2} \vec{\nabla} \times \vec{\nabla} \times (\vec{a}_z f_{N_\nu}) \tag{3}$$

and $W_{M\nu}$ and $W_{N\nu}$ are normalization constants with

$$f_{M_\nu} = \cos(k_x x)\cos(k_y y)\sin(k_z z)$$

and

$$f_{N_\nu} = \sin(k_x x)\sin(k_y y)\cos(k_z z) \tag{4}$$

$$\vec{M}_\nu(\vec{r}) = \frac{1}{k_\nu}[-\vec{a}_x k_y \cos(k_x x)\sin(k_y y) + \vec{a}_y k_x \sin(k_x x)\cos(k_y y)]\sin(k_z z) \tag{5}$$

$$\vec{N}_\nu(\vec{r}) = \frac{1}{k_\nu^2}\left\{ \begin{array}{l} [-\vec{a}_x k_x k_z \cos(k_x x)\sin(k_y y) \\ \quad - \vec{a}_y k_y k_z \sin(k_x x)\cos(k_y y)]\sin(k_z z) \\ + \vec{a}_z (k_x^2 + k_y^2)\sin(k_x x)\sin(k_y y)\cos(k_z z) \end{array} \right\}. \tag{6}$$

We can solve for the unknown current source magnitudes by using (1) to find the z-component of the electric field along the probes and setting it equal to zero. To find this component we need the scalar products of the z-directed probe currents with the M_ν and N_ν eigenvectors. But since M_ν has no z-component we do not need to evaluate the integrals J_{eM} or J_{mK} in the first term on the right of (1).

The normalization constant for the N eigenvector is

$$W_{N_\nu} = \frac{4\varepsilon_s k_\nu^2}{(k_x^2 + k_y^2)abc} \quad \text{for} \quad m, n = 1, 2, 3\cdots \text{ and } p = 0, 1, 2, 3\cdots$$
$$\varepsilon_s = \begin{cases} 1 & \text{if } p = 0 \\ 2 & \text{if } p = 1, 2, 3\cdots \end{cases}. \tag{7}$$

Let the probe currents be

$$\begin{aligned} \vec{J}_{e1} &= -\vec{a}_z I_1 \sin[k_0(z' - c + s)] \cdot \left[1 + \sigma\cos^2\left(\frac{\pi x}{w}\right)\right]\delta(y' - h_1) \\ &\quad \text{for} \quad c > z' > c - s \\ \vec{J}_{e2} &= -\vec{a}_z I_2 \sin[k_0(z' - s)] \cdot \left[1 + \sigma\cos^2\left(\frac{\pi x}{w}\right)\right]\delta(y' - h_2) \\ &\quad \text{for} \quad s > z' > 0. \end{aligned} \tag{8}$$

We have for the probe current coupling factors to the TM modes

$$J_{eN_\nu} = \int_{V'} \vec{N}_\nu(\vec{r}') \cdot (\vec{J}_{e1} + \vec{J}_{e2})\, dV' = I_1 J_{eN_\nu 1} + I_2 J_{eN_\nu 2}. \tag{9}$$

Performing the integration yields

$$\begin{aligned} J_{eN_\nu 1} &= (-)^p Q \sin(k_y h_1) H_1 \\ J_{eN_\nu 2} &= -Q\sin(k_y h_2) H_2 \end{aligned} \tag{10}$$

where

$$Q = \frac{2k_0(k_\nu^2 - k_z^2)}{k_\nu^2(k_0^2 - k_z^2)}[\cos(k_0 s) - \cos(k_z s)]$$

and

$$H_\mu = \sin(k_x l_\mu)\sin\left(\frac{k_x w}{2}\right) \cdot \left\{ \frac{1}{k_x} + \frac{2\sigma}{4 - \left(\frac{k_x w}{\pi}\right)^2}\left[\frac{1}{k_x} - \frac{w}{\pi}\sin\frac{\pi l_\mu}{w} \cdot \left(\cos\frac{\pi l_\mu}{w}\cot(k_x l_\mu) + \frac{k_x w}{2\pi}\sin\frac{\pi l_\mu}{w}\right)\right]\right\}.$$

The magnetic currents flowing over the port aperture regions have been derived as follows. The potential distribution for the shielded microstrip geometry can be described by two infinite series, $\phi_0(x, y)$ for the air dielectric region and $\phi_1(x, y)$ for the solid dielectric region [8], where

$$\phi_0(x, y) = \sum_{n\,\text{odd}} d_n \sinh \frac{n\pi(y-b)}{a} \cos \frac{n\pi x}{a}$$

and

$$\phi_1(x, y) = \sum_{n\,\text{odd}} c_n \sinh \frac{n\pi y}{a} \cos \frac{n\pi x}{a}$$

the summations being taken over odd values of n only.

The relations between the constants c_n and d_n are determined by the requirement that $\phi_0(x, d) = \phi_1(x, d)$ be satisfied independently by each of the terms of the series. The value of either constant can be determined by solving the integral equation for the charge density distribution over the width of the strip conductor. For this analysis, the assumption that the charge density is approximated by a cosine-squared distribution results in the following set of constants

$$c_n = 2\,\frac{(4C_0 a_a^2 - n^2 w^3 \rho_0) g_n}{n k_a w (4a_a^2 - n^2 w^2) \sinh(n k_a d)}$$

where

$$\rho_0 = \frac{4C_0 a_a^2}{w^3} \frac{\sum_{n\,\text{odd}} \left\{ \frac{g_n}{n(4a_a^2 - n^2 w^2)} \sin\left(\frac{n k_a w}{2}\right) \right\} - \frac{k_a}{2}}{\sum_{n\,\text{odd}} \frac{n g_n}{4a^2 - n^2 w^2} \sin\left(\frac{n k_a w}{2}\right)}$$

and

$$g_n = \frac{2}{n\pi\varepsilon_0} \frac{1}{\varepsilon_r \coth(n k_a d) - \coth[n k_a (b-d)]}$$

and ε_r is the relative dielectric constant of the solid dielectric region.

The electric field is then found from $-\vec{\nabla}\phi_0$ and $-\vec{\nabla}\phi_1$, and the magnetic currents covering the lower region (region 1) of the apertures become

$$\begin{aligned} \frac{\vec{J}_{m1\mu}}{V_\mu} &= (-)^{\mu-1} \vec{a}_z \times \frac{\vec{E}_{1\mu}}{V_\mu} \\ &= (-)^{\mu-1} \sum_{n=1,3}^{9} c_n n k_a [\vec{a}_y \sinh(n k_a y_a) \sin(n k_a x_a) \\ &\quad + \vec{a}_x \cosh(n k_a y_a) \cos(n k_a x_a)] \end{aligned} \tag{11}$$

and those covering the upper region (region 0) become

$$\begin{aligned} \frac{\vec{J}_{m0\mu}}{V_\mu} &= (-)^{\mu-1} \vec{a}_z \times \frac{\vec{E}_{0\mu}}{V_\mu} \\ &= (-)^{\mu-1} \sum_{n=1,3}^{9} d_n \\ &\quad \cdot \begin{bmatrix} \vec{a}_y \sinh[n k_a (y_a - b_a)] \sin(n k_a x_a) \\ + \vec{a}_x \cosh[n k_a (y_a - b_a)] \cos(n k_a x_a) \end{bmatrix} \end{aligned} \tag{12}$$

with $d_n = c_n \{\sinh(n k_a d)/\sinh[n k_a (d - b_a)]\}$ where x_a and y_a are the coordinates of the aperture and μ is 1 for port 1 ($z = c$) and 2 for port 2 ($z = 0$). These transform into x and y, the coordinates of the cavity, as $x_a = (-)^\mu (x - l_\mu)$, $y_a = y - h_\mu + d$.

The "magnetic" eigenvector, F_ν, is given by $\vec{F}_\nu = 1/(k_\nu)\vec{\nabla} \times \vec{N}_\nu$ whence

$$\begin{aligned} \vec{F}_\nu = \frac{1}{k_\nu} [&\vec{a}_x k_y \sin(k_x x) \cos(k_y y) \cos(k_z z) \\ &- \vec{a}_y k_x \cos(k_x x) \sin(k_y y) \cos(k_z z)]. \end{aligned} \tag{13}$$

The aperture current coupling factors then become

$$\begin{aligned} J_{mF_\nu} &= \int_{V'} \vec{F}_\nu(\vec{r}') \cdot (\vec{J}_{m1} + \vec{J}_{m2})\, dV' \\ &= \sum_\mu V_\mu J_{mF_\nu\mu} \quad \text{where} \quad J_{mF_\nu\mu} \\ &= \int_{l_\mu-(a_a/2)}^{l_\mu+(a_a/2)} \left\{ \int_{h_\mu-d}^{h_\mu} \vec{F}_\nu(\vec{r}') \cdot \vec{J}_{m1\mu}(\vec{r}')\, dx' \right. \\ &\quad \left. + \int_{h_\mu}^{h_\mu+b_a-d} \vec{F}_\nu(\vec{r}') \cdot \vec{J}_{m0\mu}(\vec{r}')\, dx' \right\} dy'. \end{aligned}$$

Substituting from (11), (12), and (13) and performing the integrations yields

$$\begin{aligned} J_{mF_\nu 1} &= \sum_{n=1,3}^{9} J_{mF_\nu 1n} \quad \text{where} \quad J_{mF_\nu 1n} \\ &= (-)^{p+1} A_{1n} B_n \sin(k_x l_1) \cos\left(\frac{k_x a_a}{2}\right) \\ J_{mF_\nu 2} &= \sum_{n=1,3}^{9} J_{mF_\nu 2n} \quad \text{where} \quad J_{mF_\nu 2n} \\ &= A_{2n} B_n \sin(k_x l_2) \cos\left(\frac{k_x a_a}{2}\right) \end{aligned} \tag{14}$$

and where

$$\begin{aligned} A_{\mu n} = \sin[k_y (h_\mu - d)] &+ \{\sinh(n k_a d) \sin[k_y (h_\mu - d + b_a)] \\ &- \sinh(n k_a b_a) \sin(k_y h_\mu)\}/ \\ &\{\sinh[n k_a (b_a - d)]\} \end{aligned}$$

and

$$B_n = \frac{2n^2 k_a^2 (k_y^2 - k_x^2) c_n}{k_\nu [k_x^2 - n^2 k_a^2][n^2 k_a^2 + k_y^2]}.$$

There are four coefficients to be evaluated: I_1, I_2, V_1, and V_2. We specify V_1 to be 1 volt, leaving three undetermined coefficients. Three moment equations involving the tangential electric field on the probes need to be established to provide a solution for the three unknowns. For the moment equations we choose the following testing functions

$$\begin{aligned} f1(x, y, z) &= \delta(x - l_1)\, \delta(y - h_1) u(z - c + s) \\ f2(x, y, z) &= \delta(x - l_2)\, \delta(y - h_2)[1 - u(z - a_s s)] \\ f3(x, y, z) &= \delta(x - l_2)\, \delta(y - h_2)[u(z - a_s s) - u(z - s)] \end{aligned}$$

where a_s is a suitable fraction. Applying these to (1) for the z-component of electric field will provide three expressions for the tangential field integrated along the input and output microstrip probes, which must vanish. Since the only functions of position will be the eigenfunctions, these are the only functions to be integrated. The eigenfunction integrals are readily evaluated to yield

$$\begin{aligned}\overline{N}_{\nu z1} &= W_{N_\nu}\int_V N_{\nu z}(x,\,y,\,z)f1(x,\,y,\,z)\,dV\\ &= (-)^p\frac{4\varepsilon_s}{k_z abc}\sin(k_x l_1)\sin(k_y h_1)\sin(k_z s)\\ \overline{N}_{\nu z2} &= W_{N_\nu}\int_V N_{\nu z}(x,\,y,\,z)f2(x,\,y,\,z)\,dV\\ &= \frac{4\varepsilon_s}{k_z abc}\sin(k_x l_2)\sin(k_y h_2)\sin(k_z s)\\ \overline{N}_{\nu z3} &= W_{N_\nu}\int_V N_{\nu z}(x,\,y,\,z)f3(x,\,y,\,z)\,dV\\ &= \frac{4\varepsilon_s}{k_z abc}\sin(k_x l_2)\sin(k_y h_2)\begin{bmatrix}\sin(k_z s)\\ -\sin(k_z a_s s)\end{bmatrix}.\end{aligned} \tag{16}$$

The three equations that result from this process are

$$\begin{vmatrix} a_{11} & a_{12} & a_{13}\\ a_{21} & a_{22} & a_{23}\\ a_{31} & a_{32} & a_{33}\end{vmatrix}\begin{vmatrix}\dfrac{I_1}{j\omega\varepsilon}\\ \dfrac{I_2}{j\omega\varepsilon}\\ -V_2\end{vmatrix} = \begin{vmatrix} b_1\\ b_2\\ b_3\end{vmatrix} \tag{17}$$

where the elements of the A matrix are given by

$$\begin{aligned} a_{11} &= \sum_\nu \kappa_\nu k_\nu J_{eN_\nu 1}\overline{N}_{\nu z1}\\ a_{12} &= \sum_\nu \kappa_\nu k_\nu J_{eN_\nu 2}\overline{N}_{\nu z1}\\ a_{13} &= \sum_\nu \kappa_\nu J_{mF_\nu 2}\overline{N}_{\nu z1}\\ a_{21} &= \sum_\nu \kappa_\nu k_\nu J_{eN_\nu 1}\overline{N}_{\nu z2}\\ a_{22} &= \sum_\nu \kappa_\nu k_\nu J_{eN_\nu 2}\overline{N}_{\nu z2}\\ a_{23} &= \sum_\nu \kappa_\nu J_{mF_\nu 2}\overline{N}_{\nu z2}\\ a_{31} &= \sum_\nu \kappa_\nu k_\nu J_{eN_\nu 1}\overline{N}_{\nu z3}\\ a_{32} &= \sum_\nu \kappa_\nu k_\nu J_{eN_\nu 2}\overline{N}_{\nu z3}\\ a_{33} &= \sum_\nu \kappa_\nu J_{mF_\nu 2}\overline{N}_{\nu z3}\end{aligned}$$

and the elements of the B vector are given by

$$\begin{aligned} b_1 &= \sum_\nu \kappa_\nu J_{mF_\nu 1}\overline{N}_{\nu z1}\\ b_2 &= \sum_\nu \kappa_\nu J_{mF_\nu 1}\overline{N}_{\nu z2}\\ b_3 &= \sum_\nu \kappa_\nu J_{mF_\nu 1}\overline{N}_{\nu z3}.\end{aligned}$$

The total probe current flowing into the input probe is found by integrating the surface current density I_1 over the width of the probe. This yields $I_T = I_1 w[1 + (\sigma/2)]\sin(k_0 s)$. Finally, the S-parameters in terms of I_T and V_2 and isolation become

$$\begin{aligned} S_{11} &= \frac{1 - Z_{0L}I_T}{1 + Z_{0L}I_T}\\ S_{21} &= \frac{2V_2}{1 + Z_{0L}I_T}\end{aligned}$$

and

$$\text{Isolation} = -20\log S_{21}. \tag{18}$$

These equations were derived under the assumption that the ports are in opposite sides of the cavity and that the probes are terminated in open circuits. If, instead, the ports are in adjacent sides of the cavity, the coupling between the ports would still be via the TM cavity modes and a procedure similar to that above could be used to compute the coupling. If the probes are terminated in their characteristic impedance, considering them to be transmission lines, there will be no current reflected from the tips of the probes. In this case the currents can be assumed to be uniform in magnitude along the probes. Taking this into account, (8) can be accordingly altered, and (10) can be replaced by somewhat different coupling factors for the electric currents.

III. Cavity Isolation Computations

The analytical method described here has been used to predict the isolation between ports 1 and 2 for a specific design of cavity and shielded microstrip ports. The cavity dimensions used for the computations are the following

$$\begin{aligned} a &= 9.652\text{ mm}\\ b &= 0.889\text{ mm}\\ c &= 14.859\text{ mm}.\end{aligned}$$

The following are the aperture dimensions used

$$\begin{aligned} l_1 &= l_2 = 3.175\text{ mm}\\ d &= h = 0.254\text{ mm}\\ a_a &= 1.321\text{ mm}\\ b_a &= 0.889\text{ mm}\\ w &= 0.229\text{ mm}.\end{aligned}$$

The microstrip conductors extend into the cavity as probes for a distance of 1.016 mm.

The computations were programmed into MathSoft's MATHCAD software on a 486 PC. Each computation at a single frequency took about four minutes. The summations over the mode index ν, which comprises the three indexes m, n, and p, involve triple summations. For the matrix elements representing the effect of a particular source on the electric field at the other end of the cavity, e.g., a_{12}, the series summed over p are alternating. They produce very small numbers, the computation of which requires a large number of terms for accuracy and is plagued by round-off errors. Fortunately these summations can be replaced with closed-form expressions by the application of partial fractions and Poisson summation theory [9] or directly from tabulated series [10]. Appendix A presents the results of these replacements.

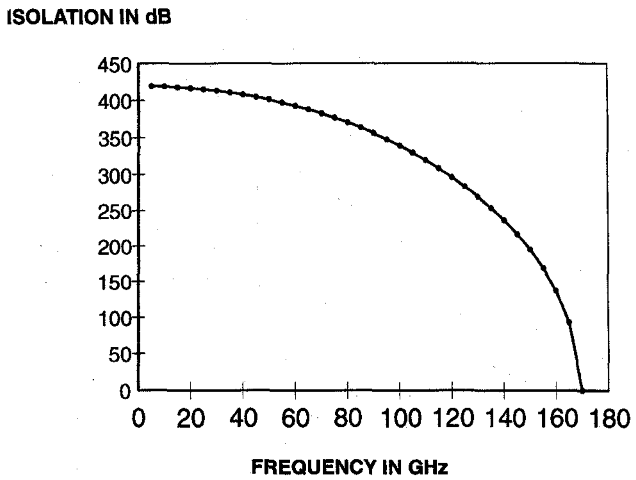

Fig. 2. Predicted frequency-dependence of isolation for a prototype MMIC package.

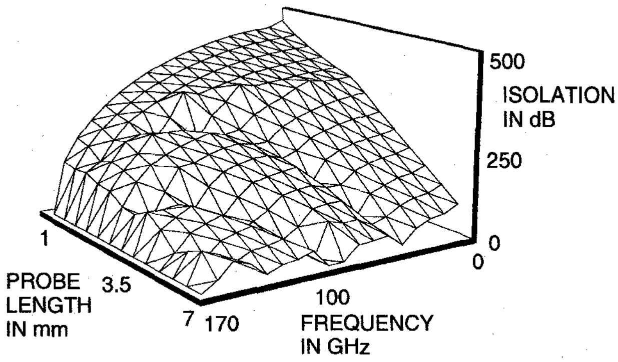

Fig. 3. Dependence of isolation on probe length and frequency.

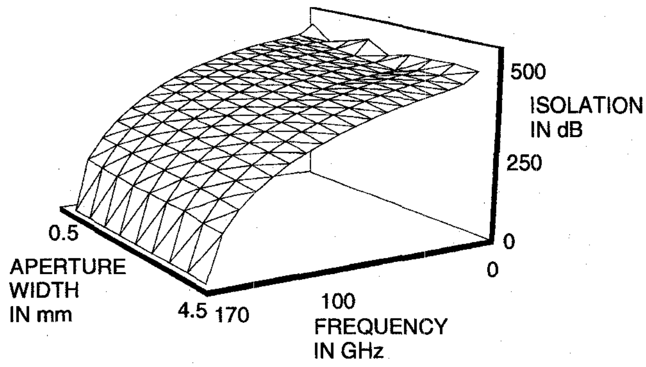

Fig. 4. Dependence of isolation on aperture width and frequency.

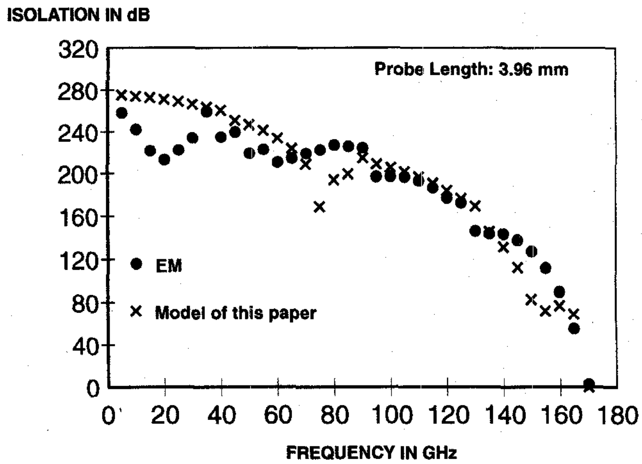

Fig. 5. Comparison of isolation predictions from this model with those from commercial software package EM.

Fig. 2 displays the frequency-dependence of the isolation computed with the model for the dimensions given above over a wide range of frequency. The summations were truncated when m and n reached 50 and 25, respectively. Note that the isolation slumps off to near zero at about 170 GHz, which is the lowest of the resonance frequencies for the TM modes.

Figs. 3 and 4 are surface plots, which show how the frequency-dependence of isolation varies with probe length, s, and with aperture width, a_a, respectively.

IV. Comparison of Computed Data with Data from Other Sources

Attempts were made to confirm the predictions of the model with sample cavities that simulated actual packages. These consisted of two coaxial lines with SMA connectors soldered into opposite walls of a short length of X-band waveguide short-circuited at both ends. The attempts to measure the isolation between input and output lines with a HP 8510 network analyzer proved futile. To measure such large values of isolation is beyond the capability of such an instrument and would have required a sensitive radio receiver, which was not available.

Instead, the predictions of the model were compared with those produced with the aid of a recognized commercial software package: Sonnet Corporation's EM software run on a Sun SparcStation. In analyzing coupling between probes in a cavity the model described here is best suited to short probe lengths, because of using only a single expansion function to approximate the current distribution along the probes. On the other hand, EM is best suited to analyzing long probe lengths with small gaps. Therefore, a compromise between these two extremes was needed. As a compromise a probe length of 3.96 mm was chosen for the comparison. A value of 9.7 for alumina was used as the relative dielectric constant, ε_r. The values produced by both EM and this program are plotted in Fig. 5. As is apparent the agreement is quite close. This may be a bit surprising considering that EM's model is based on the assumption that the ports are coaxial lines and are modeled simply as voltages with fixed capacitors from the edges of the signal conductor pattern to the surrounding metal box.

V. Conclusion

A computer model has been created for predicting the isolation between RF ports of a class of MMIC packages that approximate a rectangular cavity with shielded microstrip ports at opposite ends. The model has been used to predict isolation using MathSoft's MATHCAD 4.0 software package on a 486 PC. From comparisons with a commercial software package, the model appears to give reasonably accurate predictions of isolation. Although it predicts coupling to cavity modes that are TM to the axis of the ports, it does not predict coupling to the TE modes, because of the simplified assumptions used in deriving the model. The latter modes are ordinarily only weakly excited, but their resonance frequencies are much lower than those of the TM modes for conventional package designs.

The actual isolation of the ports in a MMIC package depends not only on coupling through the interior of the package, as modeled here, but also on coupling via the ceramic or plastic walls and on signal leakage around the exterior of the package. Coupling through these latter paths may actually be the dominant contributors to the total coupling between ports. Certainly the isolation predicted by the model described here is far beyond what should be required for good MMIC performance.

ACKNOWLEDGMENT

The author would like to acknowledge the continuing encouragement, valuable suggestions, and helpful discussions received from Prof. D. R. Decker of Lehigh University. The assistance to the author by Mrs. R. Tatikola, also of Lehigh, in dealing with the frustrations of computer utilization is also much appreciated.

APPENDIX A

As stated in the body of the paper, the computations of isolation were both shortened and made more accurate by the conversion of the summations with respect to the index p into closed-form expressions. In general, slowly converging infinite series can often be transformed into more rapidly converging series by the application of Poisson summation theory [9]. Sometimes one is fortunate to be able to replace an infinite series by simply a closed-form expression. This happened to be the case with the summations in question.

First, it was necessary to separate the fractions into sets of partial fractions. This resulted in the decomposition of a single series into the sum of two or three separate infinite series. Equivalent closed-form expressions for these series, as it happens, are listed in Gradshteyn and Ryzhik [10]. The results of these transformations are presented below.

For matrix element a_{11}

$$\sum_{p=1}^{\infty} \frac{[\cos(k_0 s) - \cos(k_z s)]\sin(k_z s)}{(k_\nu^2 - k_0^2)(k_0^2 - k_z^2)k_z} = \frac{1}{2r_{xy}^2}\left\{\frac{(c-s)[\cos(k_0 s) - 1]}{k_0^2} + \frac{c[\cos(k_0 s) - \cosh(r_{xy}s)]\sinh[r_{xy}(c-s)]}{q_{xy}^2\sinh(r_{xy}c)}\right\}$$

$$\text{where } q_{xy} = \sqrt{k_x^2 + k_y^2} \text{ and } r_{xy} = \sqrt{q_{xy}^2 - k_0^2}. \tag{A1}$$

For matrix element a_{12}

$$\sum_{p=1}^{\infty} (-)^p \frac{[\cos(k_0 s) - \cos(k_z s)]\sin(k_z s)}{(k_\nu^2 - k_0^2)(k_0^2 - k_z^2)k_z} = \frac{1}{2r_{xy}^2}\left\{\frac{s[1 - \cos(k_0 s)]}{k_0^2} + \frac{c[\cos(k_0 s) - \cosh(r_{xy}s)]\sinh(r_{xy}s)}{\sinh(r_{xy}c)}\right\} \tag{A2}$$

with similar expressions for a_{21}, a_{22}, a_{31}, and a_{32}.

For matrix element a_{13}

$$\sum_{p=1}^{\infty} (-)^p \frac{\sin(k_z s)}{(k_\nu^2 - k_0^2)k_z} = \frac{1}{2r_{xy}^2}\left[\frac{c\sinh(r_{xy}s)}{\sinh(r_{xy}c)} - s\right]. \tag{A3}$$

For vector element b_1

$$\sum_{p=1}^{\infty} \frac{\sin(k_z s)}{(k_\nu^2 - k_0^2)k_z} = \frac{1}{2r_{xy}^2}\left\{c - s - \frac{c\sinh[r_{xy}(c-s)]}{\sin h(r_{xy}c)}\right\} \tag{A4}$$

with similar expressions for matrix elements a_{23} and a_{33} and vector elements b_2 and b_3.

REFERENCES

[1] J. Liang, H. Chang, and K. A Zaki, "Coaxial probe modeling in waveguides and cavities," *IEEE Trans. Microwave Theory Tech.*, vol. 40, pp. 2172–2180, Dec. 1992.
[2] J. M. Jarem, "A multifilament method-of-moments solution for the input impedance of a probe-excited semi-infinite waveguide," *IEEE Trans. Microwave Theory Tech.*, vol. MTT-35, pp. 14–19, Jan. 1987.
[3] B. Wong, "Mutual impedance between probes in a waveguide," *IEEE Trans. Microwave Theory Tech.*, vol. MTT-36, pp. 53–59, Jan. 1988.
[4] R. F. Harrington, *Time-Harmonic Electromagnetic Fields.* New York: McGraw-Hill, ch. 3, 1961.
[5] M. Kisliuk, "The dyadic Green's functions for cylindrical waveguides and cavities," *IEEE Trans. Microwave Theory Tech.*, vol. MTT-28, pp. 894–898, Aug. 1980.
[6] R. F. Harrington, *Time-Harmonic Electromagnetic Fields.* New York: McGraw-Hill, ch. 8, 1961.
[7] R. E. Collin, *Field Theory of Guided Waves,* 2nd ed. New York: IEEE Press, ch. 7, 1991.
[8] R. C. Booton, Jr., *Computational Methods for Electromagnetics and Micro-waves.* New York: Wiley, 1992, ch. 10.
[9] P. R. Wallace, *Mathematical Analysis of Physical Problems.* Mineola, NY: Dover, 1984, p. 169.
[10] I. S. Gradshteyn and I. M. Ryzhik, *Table of Integrals, Series, and Products.* London: Academic, pp. 38 and 40.

Hilding M. Olson (S'48–M'53–LM'90) was born in Crystal Lake, IL. He received the B.S.E.E. degree from Northwestern University, Evanston, IL, the M.S. degree in electrical engineering from Stevens Institute of Technology, Hoboken, NJ, and the D.E.E. degree from Polytechnic Institute of Brooklyn (now Polytechnic University) in 1948, 1954, and 1959, respectively.

From 1948 to 1953, he was with Radio Corporation of America. From 1953 to 1987, he was with AT&T Bell Laboratories where he was a Group Supervisor. Since 1987, he has been Visiting Research Scientist with Lehigh University, Bethlehem, PA. His research interests are in microwave packaging, computational electromagnetics, and computer software for designing microwave devices.

Dr. Olson is a member of Tau Beta Pi, Eta Kappa Nu, and Sigma Xi.